International Journal of
*Molecular Sciences*

MDPI

*Supplementary materials*

# Impact of HLA-DR Antigen Binding Cleft Rigidity on T Cell Recognition

**Christopher Szeto [1,†], Joseph I. Bloom [1,†], Hannah Sloane [1], Christian A. Lobos [1], James Fodor [1,2], Dhilshan Jayasinghe [1], Demetra S. M. Chatzileontiadou [1], Emma J. Grant [1], Ashley M. Buckle [1] and Stephanie Gras [1,3,*]**

[1] Department of Biochemistry and Molecular Biology, Biomedicine Discovery Institute, Monash University, Clayton, VIC 3800, Australia; chris.szeto@monash.edu (C.S.); joseph.i.bloom@gmail.com (J.I.B.); hslo1@student.monash.edu (H.S.); christian.lobos@monash.edu (C.A.L.); fods12@gmail.com (J.F.); dhilshan.jayasinghe@monash.edu (D.J.); dimitra.chatzileontiadou@monash.edu (D.S.M.C.); emma.grant@monash.edu (E.J.G.); ashley@ptngconsulting.com (A.M.B.)

[2] Eccles Institute of Neuroscience, John Curtin School of Medical Research, The Australian National University, Canberra, ACT 0200, Australia

[3] Australian Research Council Centre of Excellence for Advanced Molecular Imaging, Monash University, Clayton, VIC 3800, Australia

* Correspondence: Stephanie.gras@monash.edu

† These authors contribution equally.

| Residue | HLA-DR11 | HLA-DR15 | HLA-DR1 |
|---|---|---|---|
| 9 | E | W | W |
| 10 | Y | Q | Q |
| 11 | S | P | L |
| 12 | T | K | K |
| 13 | S | R | F |
| 26 | F | F | L |
| 28 | D | D | E |
| 30 | Y | Y | C |
| 31 | F | F | I |
| 37 | Y | S | S |
| 47 | F | F | Y |
| 58 | E | A | A |
| 67 | F | I | L |
| 70 | D | Q | Q |
| 71 | R | A | R |
| 96 | H | Q | E |
| 133 | R | L | R |
| 140 | T | A | A |
| 142 | V | M | V |
| 149 | H | Q | Q |

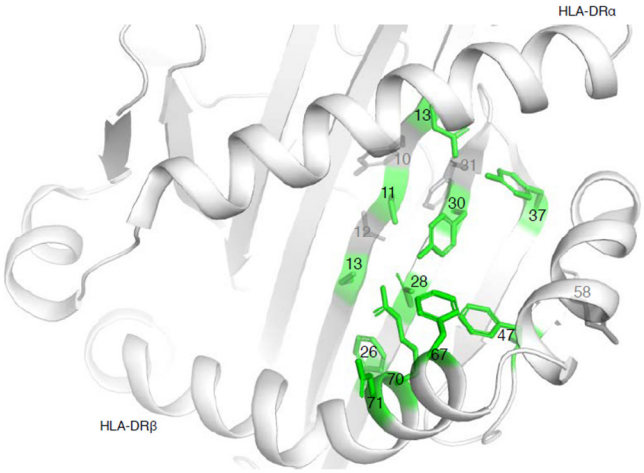


**Figure S1.** Polymorphic residues in HLA-DR antigen binding cleft. Crystal structure of HLA-DR11-RQ13 (PDB ID: 6CPN) (white) showing polymorphic residues (as sticks) that face towards (green) or face away (grey) from the antigen binding cleft. The table indicates the nature of the polymorphic residues among HLA-DR11, HLA-DR15 and HLA-DR1 molecules, and are coloured green if they are facing towards the peptide binding cleft.

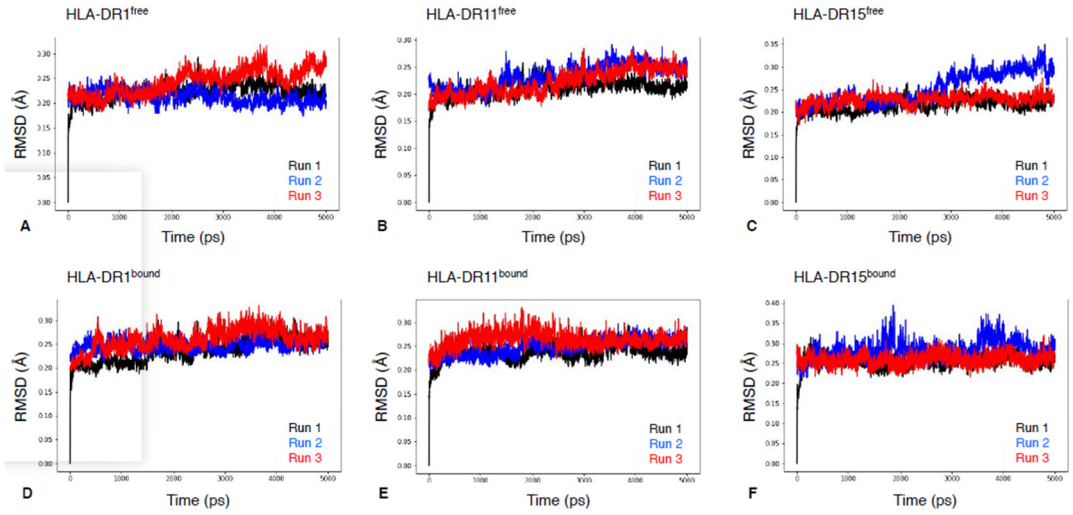


**Figure S2.** MD RMSD plots for HLA-DR molecules. MD RMSD plots for triplicate simulations over a 500 ns timeframe for HLA-DR molecules (**A**) HLA-DR1$^{free}$, (**B**) HLA-DR11$^{free}$, (**C**) HLA-DR15$^{free}$, (**D**) HLA-DR1$^{bound}$, (**E**) HLA-DR11$^{bound}$, and (**F**) HLA-DR15$^{bound}$. RMSD calculations are relative to the first frame of the first run.

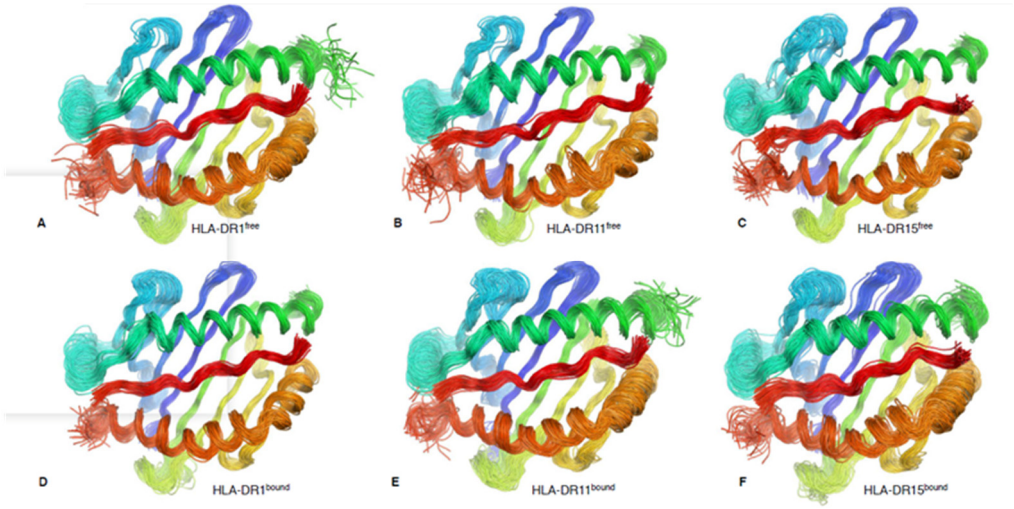


**Figure S3.** Structural overlay of MD simulations. MD structures taken from 500 ns triplicate simulations were overlayed for (**A**) HLA-DR1$^{free}$, (**B**) HLA-DR11$^{free}$, (**C**) HLA-DR15$^{free}$, (**D**) HLA-DR1$^{bound}$, (**E**) HLA-DR11$^{bound}$, and (**F**) HLA-DR15$^{bound}$. Each structure is a snapshot taken from MD trajectory at 20 ns intervals.

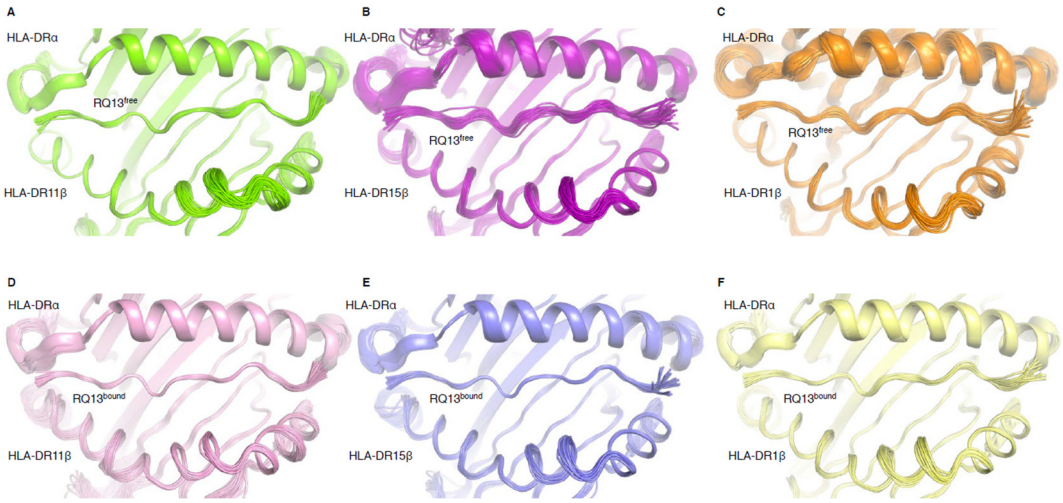


**Figure S4.** Overlay of ensemble models at the antigen binding cleft. Ensemble results of the antigen binding cleft (HLA-DR$\alpha$ represented by cartoon; HLA-DR$\beta$ and peptide as ribbon) for HLA-DR-RQ13 complexes in free (**A–C**) or F24 TCR bound (**D–F**) state. HLA-DR11-RQ13 structures are coloured in green (free, **A**) and pale pink (bound, **D**); HLA-DR15-RQ13 structures are coloured in purple (free, **B**) and blue (bound, **E**); and HLA-DR1 structures are coloured in orange (free, **C**) and yellow (bound, **F**).

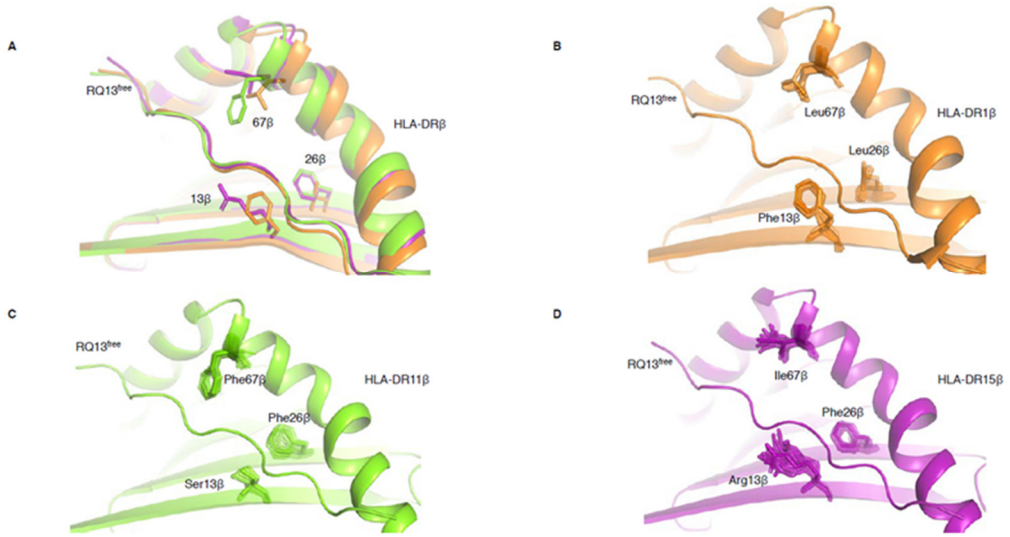


**Figure S5.** Conformational variation of polymorphic residues that open the cleft. **(A)** Structural alignment of crystal structures from HLA-DR-RQ13 complexes showing polymorphic residues HLA-DR$\beta$13, HLA-DR$\beta$26 and HLA-DR$\beta$67 (stick) that cause the cleft to open. (**B** to **C**) Ensemble results of the same polymorphic residues for (**B**) HLA-DR11-RQ13 (**C**) HLA-DR15-RQ13 and (**D**) HLA-DR1-RQ13.

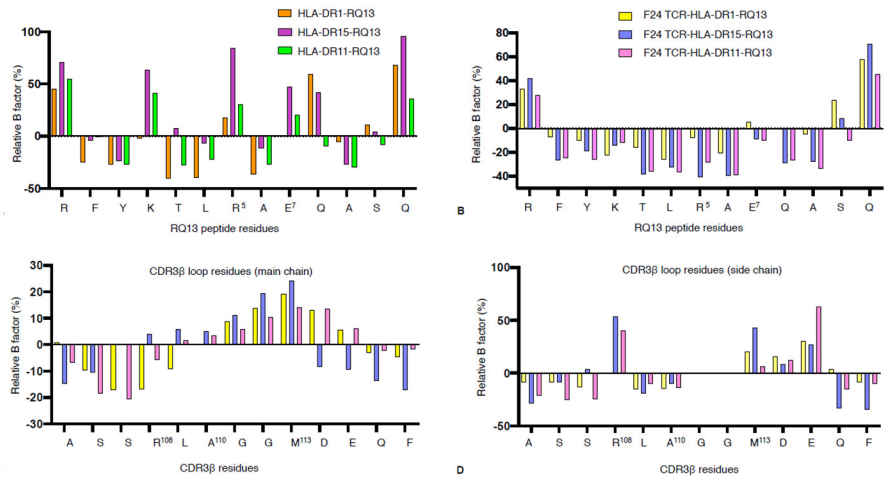


**Figure S6.** Relative B factor analysis of RQ13 peptide and CDR3β loop from the crystallographic structures. The relative B factor was calculated for the side chain of the RQ13 peptide residues from the HLA-DR-RQ13 structures in their free (**A**) and bound (**B**) states. The relative B factor (%) is calculated with the side chain average B factor [100 × (($B_{residue}$ – $B_{cleft}$)/$B_{cleft}$))] and represented as coloured bar for each structures. (**A**) The bars are coloured in orange for HLA-DR1-RQ13, green for HLA-DR11-RQ13, and pink for HLA-DR15-RQ13 structures in their free state, or yellow, pale purple, pale pink in their bound state (**B**), respectively. For (**C**) and (**D**) panels, the relative B factor is calculated with the main chain (**C**) or side chain (**D**) of each residue of the F24 TCR CDR3β loop [100 × (($B_{residue}$ – $B_{CDR3β}$)/$B_{CDR3β}$))].

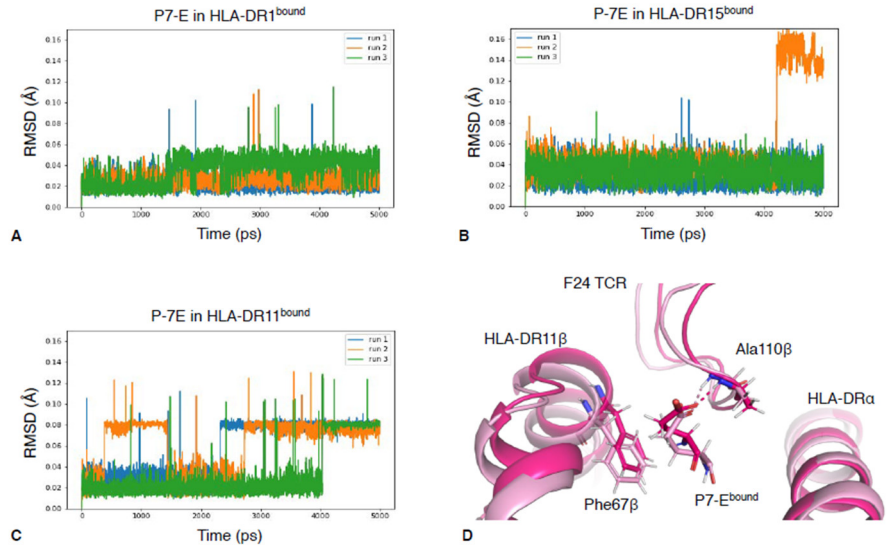


**Figure S7.** MD RMSD for P7-E side chain in HLA-DR$^{bound}$ simulations. MD RMSD plots for triplicate simulations over a 500 ns timeframe for TCR-bound HLA-DR molecules for P7-E in (**A**) HLA-DR1, (**B**) HLA-DR15, (**C**) HLA-DR11. RMSD calculations are relative to the first frame of the first run. (**D**) Structural alignment of HLA-DR11$^{bound}$ taken from Run 2 between frame 1500 (pink) and 4900 (dark pink) showing two structural conformations of P7-E forming a hydrogen bond with Ala110β (dashed line) with a bond distance of 2.2 Å and 1.8 Å, respectively.

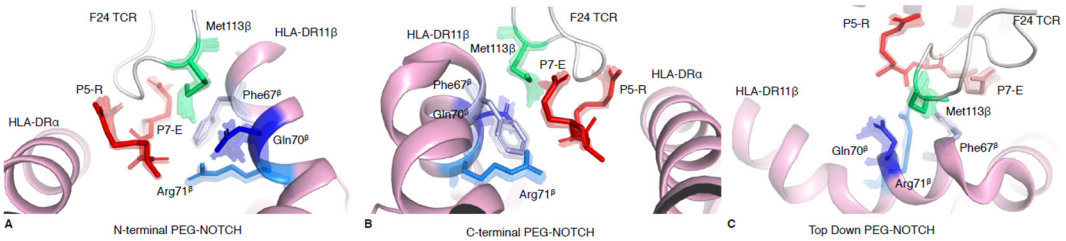


**Figure S8.** Spatial variation of residues that form the peg-notch interaction. The peg-notch interaction is driven by F24 TCRβ loop (white) Met113β (turquoise) that inserts itself into the notch formed by HLA-DR11-RQ13 (light pink). Each panel shows the same peg-notch interaction from the point of view of (**A**) the N-terminus (**B**) the C-terminus and (**C**) a top-down TCR perspective. The RQ13 peptide residues at position 5 and 7 are represented as red sticks, while HLA-DR11 residue Phe67β, Gln70β and Arg71β are represented as blue sticks.

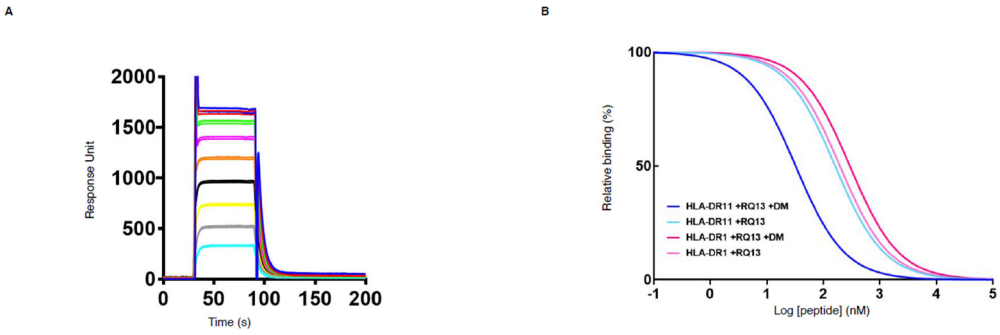


**Figure S9.** SPR and peptide binding exchange assays. (**A**) F24 TCR binding kinetics to HLA-DR1-D66A$^{\beta}$ mutant presenting RQ13 peptide determined by SPR. The curves represent the concentration range used of F24 TCR. (**B**) The displacement of HA$_{TAMRA}$ peptide by increasing concentrations of RQ13 peptide. The shift in binding curves of HLA-DR11 (light blue) indicates that the addition of HLA-DM facilitates displacement of HA$_{TAMRA}$ by RQ13 peptide (blue), whereas, HLA-DR1 (light pink) and HLA-DR1 in the presence of HLA-DM (pink) shows no shift.

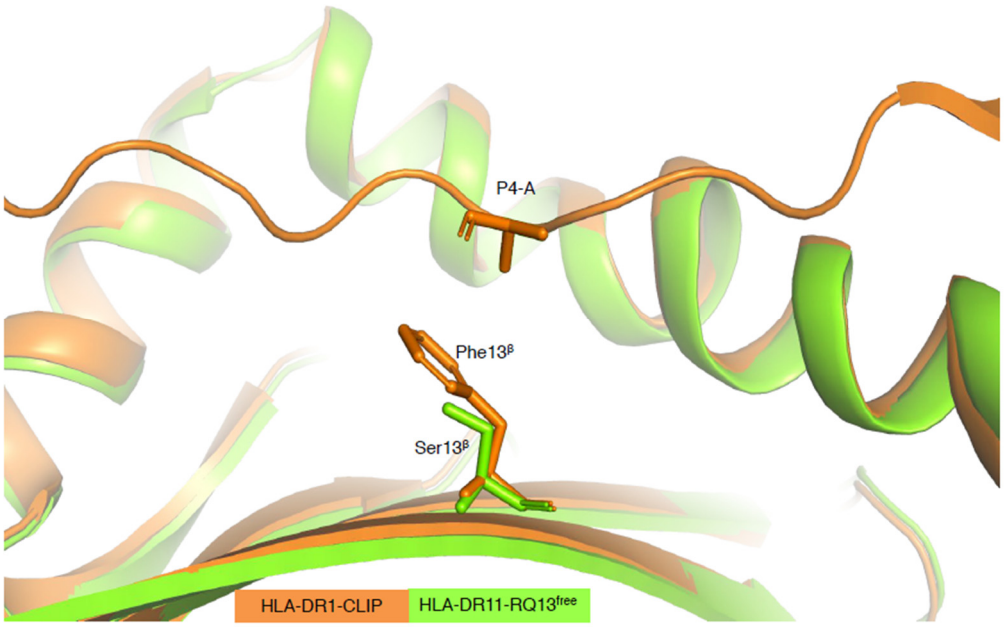


**Figure S10.** Structural alignment of HLA-DR11-RQ13 and HLA-DR1-CLIP. Crystal structure of HLA-DR1-CLIP (PDB ID: 3PDO, orange) shows that polymorphic residue Phe13β can form VdW interactions with P4-A in HLA-DR1-CLIP, but this may not be possible for Ser13β in HLA-DR11 (green).